

PMMA Coated BaF₂:Er³⁺ Nanoparticles via a Novel One-Step Reverse-Emulsion Polymerization Process

Hongzhou Lian,^{†,§} Lianshe Fu,^{†,*} Paulo S. André,[‡] and Jun Lin[§]

[†]Department of Physics, CICECO, University of Aveiro, 3810-193 Aveiro, Portugal. *E-mail: lianshefu@ua.pt

[‡]Instituto de Telecomunicações and Department of Physics, University of Aveiro, 3810-193 Aveiro, Portugal

[§]State Key Laboratory of Rare Earth Resource Utilization, Changchun Institute of Applied Chemistry, Chinese Academy of Sciences, Changchun 130022, P.R. China

Received February 19, 2013, Accepted May 22, 2013

Poly(methyl methacrylate) coated BaF₂:Er³⁺ nanoparticles were prepared via a novel reverse-emulsion polymerization process using methyl methacrylate as continuous phase and water as dispersed phase. Preparation and coating of BaF₂:Er³⁺ particles were processed in a single step. The resulting polymeric composites show the characteristic Er³⁺ luminescence at excitation of 980 nm and may have potential applications in amplified optical networks.

Key Words : Nanoparticles, Composite materials, Reverse-emulsion polymerization, Luminescence

Introduction

Due to its potential applications as optical amplifiers for the telecommunications spectral window around 1540 nm, Er³⁺ doped material are promising to compensate signal loss during transmission in optical fibers. MF₂ (M = Ca, Ba) has been proven to be a promising host for the 1540 nm emission of Er³⁺ due to its low phonon energy in contrast to oxides and to its transparency.¹⁻⁵ However, the poor solubility of lanthanide elements in pure inorganic hosts leads to clustered lanthanide ion species, which in turn has limited the amplification achievable.

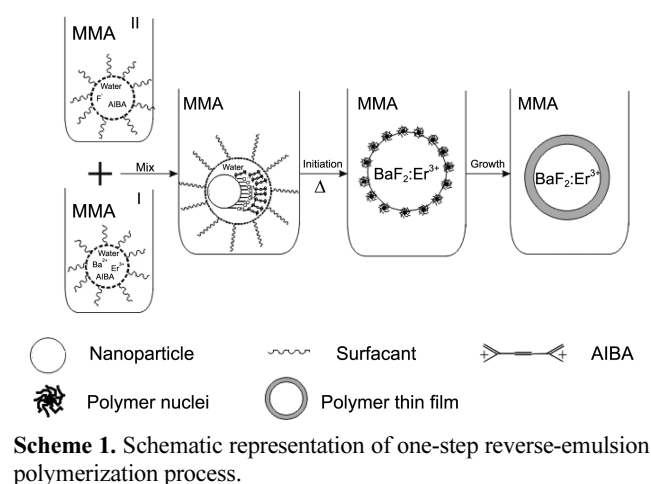
As well known, organic/inorganic composites consisting of light-amplifying nanoparticles incorporated into a polymer matrix are promising materials to circumvent these problems.⁶ BaF₂ has cubic structure and only one refractive index (1.47) and thus can be matched well with a polymer such as poly(methyl methacrylate) (PMMA) which is desired to avoid significant light scattering.⁷ The resulting films with tailed properties can be used as optical waveguide amplifier.⁸ However, inorganic particles usually have high surface energy because of their hydrophilic ionic nature, and the hydrophobic polymer does not interact well with them because of the differences in surface energy.⁹ Therefore, to improve the interfacial adhesion between the inorganic particles and the polymer matrix by modifying the inorganic particles surface becomes very important.¹⁰ Although the traditional methods of treating the inorganic particles surface could be performed using low-molecular coupling agents or two-step emulsion polymerization process,¹¹ the former has a tendency for nanoparticles to migrate out from the composites and the latter is difficult to avoid aggregation of nanoparticles. As a consequence, there is degradation in the mechanical and physical properties of composites. Therefore, to develop a method to combine BaF₂:Er³⁺ nanoparticle and polymer is very important.

Previously, we synthesized BaF₂ and BaF₂:Er³⁺ nanoparticles in a quaternary reverse micelle of cetyltrimethylammonium bromide (CTAB), *n*-butanol, *n*-octane, and water.^{12,13} In order to synthesize PMMA coated BaF₂:Er³⁺ nanoparticles, in this paper, we used methyl methacrylate (MMA) instead of *n*-octane and explored a novel one-step reverse-emulsion polymerization process, in which the preparation and coating of BaF₂:Er³⁺ nanoparticles with PMMA were carried out in one step. Unlike the traditional emulsion polymerization, in this system, the continuous phase is MMA monomer and the dispersed phase is water. We call this kind of polymerization as “reverse-emulsion polymerization”.

Experimental

Preparation of Uncoated and PMMA Coated BaF₂:Er³⁺ Nanoparticles. Based on our previous works and other literature method,¹²⁻¹⁴ the uncoated 12 mol % Er³⁺-doped BaF₂ nanoparticles (the molar ratio of BaF₂:Er³⁺ is 1:0.12) were prepared from the quaternary reverse micelles of CTAB, *n*-butanol, MMA, and water. The clear or turbid emulsions can be obtained depending on the relative quantities of the components. When the emulsions with 18.5 CTAB, 15.1 *n*-butanol, 51.8 MMA and 14.6 H₂O solution (% w/w values of components) were used, after stirring, stable microemulsions can be obtained. The aqueous phases were a mixture of 3 mmol/L Ba(NO₃)₂ and 0.36 mmol/L Er(NO₃)₃ in reverse micelle **I** and 9 mmol/L NH₄F in reverse micelle **II**. These two reverse micelles were stirred separately at room temperature until a well-distributed system was obtained, and then mixed under vigorous stirring. After 15 minute reaction, the uncoated BaF₂:Er³⁺ particles were collected by centrifugation, washed with a 1:1 mixture of methanol and dichloromethane, followed by centrifugal recovery and drying.

PMMA coated BaF₂:Er³⁺ nanoparticles were prepared using



similar process as that of uncoated nanoparticles except that an initiator 2,2'-azobis(2-methylpropionamide) dihydrochloride (AIBA) was added into the reverse micelles **I** and **II** (Scheme 1). The concentration of AIBA in the aqueous phase of microemulsion **I** and **II** is 1.25 mmol/L. After 15 minute of reaction of reverse micelles **I** and **II** under nitrogen atmosphere, the mixture was heated to 60 °C, and the polymerization process lasted for further 5 h. The PMMA coated BaF₂:Er³⁺ nanoparticles were obtained by centrifugal recovery and drying.

Preparation of BaF₂:Er³⁺/PMMA Nanocomposites. The uncoated and PMMA coated BaF₂:Er³⁺ nanoparticles were respectively dispersed into MMA monomer (5%, w/w) with AIBA as initiator, and the BaF₂:Er³⁺/PMMA nanocomposites were obtained by bulk polymerization technique. The pre-polymerization was carried out at 60 °C in ultrasonic vibration water bath and then the mixtures were cured at 60 °C until the final bulk nanocomposites were obtained.

Characterization. The phase purity was examined by powder X-ray diffraction (XRD) patterns performed on a Rigaku-Dmax 2500 diffractometer using Cu K α radiation (λ = 0.15405 nm). Transmission electron microscope (TEM) was recorded on FEI Tecnai G2 S-Twin with an acceleration voltage of 200 kV. Field emission scanning electron microscopy (FESEM) was measured on XL30 microscope (Philips). Inductively Coupled Plasma (ICP) measurement (ICP-PLASMA 1000) was used to determine the compositions. The photoluminescence spectra were obtained from InGaAs detector using 980 nm from a tunable laser as the excitation (Continuum Sunlite OPO).

Results and Discussion

Figure 1 shows XRD patterns of uncoated (a), PMMA coated BaF₂:Er³⁺ particles (b), and the standard XRD pattern of BaF₂ crystalline phase. All the peaks can be indexed to a pure cubic phase [JCPDS card No. 04-0452, space group: Fm3m(225)] of BaF₂ with lattice constant a = 6.2 Å. All the peaks confirm that the two kinds of Er³⁺-doped BaF₂ particles phase and that Er-doping and PMMA coating do

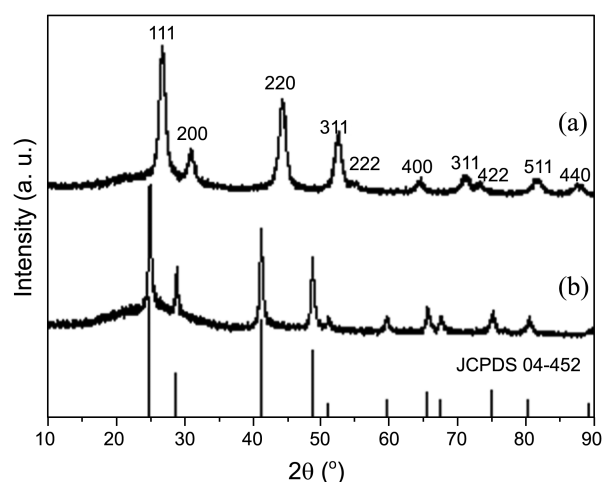


Figure 1. XRD patterns of uncoated (a) and PMMA coated (b) BaF₂:Er³⁺ nanoparticles (b).

not change the structure of BaF₂, a similar result with the literature.¹⁵ The peaks for ErF₃ are not seen in the XRD patterns, suggesting that the nanoparticles are not a core of ErF₃ surrounded by BaF₂ or nanocrystals of ErF₃ embedded in BaF₂ and that probably, Er³⁺ ions substitute partly for the Ba²⁺ and get into the lattice.¹⁶ The particle sizes can be estimated by using Scherrer formula to be 11.8 nm and 23.5 nm for uncoated and PMMA coated BaF₂:Er³⁺ particles, respectively, indicating that BaF₂:Er³⁺ particles were coated by PMMA. Compared to the standard pure BaF₂ pattern, the excursion of the diffraction peaks in Figure 1(a), which has also been found in Er³⁺-doped oxy-fluoride glass ceramics,¹⁷ is related to the size of particles, *i.e.* the smaller the particle size is, the bigger the excursion is. No pattern excursion can be observed in Figure 1(b), indicating that the particle size of PMMA coated particles is bigger than that of uncoated particles. The peaks broadening may be related with the Er³⁺ doping concentrations in the nanoparticles.¹⁶ In addition, the ICP data shows also that there are no other elements in the nanoparticles and the ratio of erbium to barium is about 12 mol%, which is consistent with the starting ratio.

Figure 2 shows the TEM images of uncoated and PMMA coated BaF₂:Er³⁺ nanoparticles. The uncoated particles are well-dispersed with size around 5 to 10 nm, while PMMA coated particles with size around 15 to 20 nm are slightly polydispersed and larger than those of uncoated particles. This result is consistent with the XRD result although the particle size observed with TEM is slightly smaller than that calculated by Scherrer formula. The difference of particle size can be attributed to the reacting time and polymer coating. The number of the nuclei formed at the very beginning of the reaction determines the size of the resultant particles.¹⁸ The collision probability between two atoms is much lower than that between one atom and a nucleus already formed, indicating that once the nuclei are formed, the growth process would be superior to the nucleation. Therefore, the atoms formed at the latter period are mainly used to the collision with the nuclei already formed instead of the

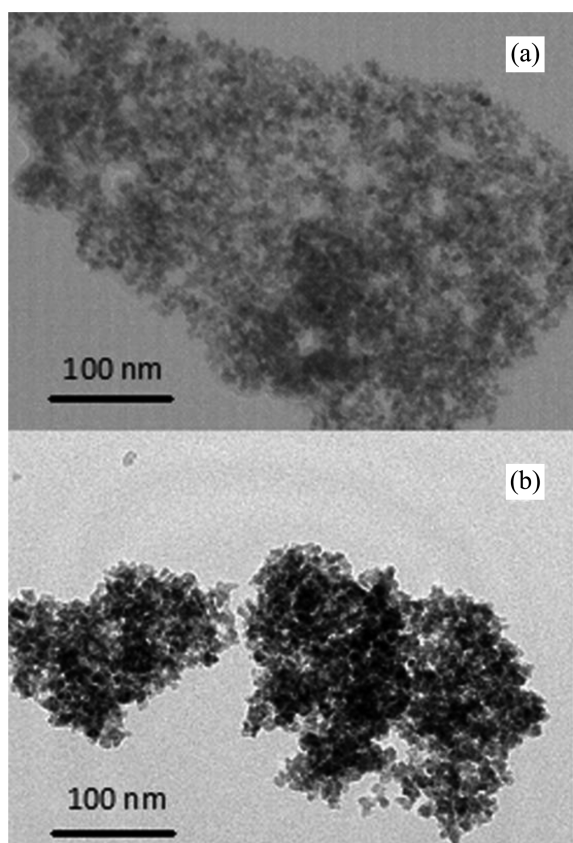


Figure 2. TEM images of uncoated (a) and PMMA coated (b) $\text{BaF}_2:\text{Er}^{3+}$ nanoparticles.

formation of new nuclei and thus leads to the formation of larger particles. The reacting time for PMMA coated particles is much longer than that of uncoated one. In the process of preparation coated particles, the atoms continue to collide with the formed nucleus after 15-minute of reaction until the surface of particles entirely coated with a layer of PMMA thin film, which prevented the collision between the atoms and the nuclei and then the growth process of crystal ended. In addition, the coating of polymer film can also lead to increase particle size as observed from TEM.

Figure 3 presents the FESEM images of uncoated (a) and PMMA coated nanoparticles/PMMA composites (b). They show very different morphologies. For the uncoated nanoparticles in PMMA composites, it is hard to find $\text{BaF}_2:\text{Er}^{3+}$ nanoparticles on the surface (Figure 3(a)), while the well dispersion of PMMA coated nanoparticles in the matrix can be seen (Figure 3(b)). This is probably related to the surface properties of the nanoparticles. As well known, the surfaces of the uncoated $\text{BaF}_2:\text{Er}^{3+}$ nanoparticles are hydrophilic. After coated by PMMA, their surfaces changed to hydrophobic. Based on the principle of “like dissolves like,” the PMMA coated $\text{BaF}_2:\text{Er}^{3+}$ nanoparticles can disperse more uniformly in MMA monomer solution than uncoated nanoparticles, thus resulting in more uniformly dispersed $\text{BaF}_2:\text{Er}^{3+}$ nanoparticles in PMMA coated nanoparticles/PMMA composites than in uncoated nanoparticles/PMMA composites. In the meanwhile, the PMMA coated $\text{BaF}_2:\text{Er}^{3+}$

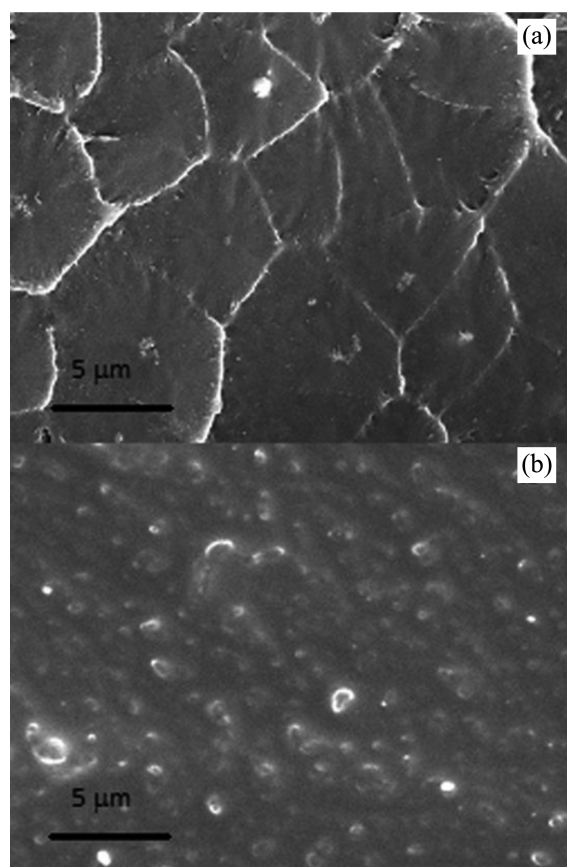


Figure 3. FESEM images of uncoated (a) and PMMA coated (b) $\text{BaF}_2:\text{Er}^{3+}$ /PMMA nanocomposites.

nanoparticles can also behave as nuclei for further polymerization, resulting in the formation of larger particles in PMMA composites than the corresponding PMMA coated nanoparticles that observed from TEM images.

The photoluminescence spectra of uncoated nanoparticles (a), PMMA coated nanoparticles (b), uncoated nanoparticles/PMMA composites (c) and PMMA coated nanoparticles/PMMA composites (d) are shown in Figure 4. By excitation at 980 nm, all the spectra show a broad emission centered at 1535 nm, which is attributed to the transition from the first excited state ($^4\text{I}_{13/2}$) to the ground state ($^4\text{I}_{15/2}$) of Er^{3+} . From the emission spectra, we can see all the bands can be deconvoluted into several peaks, indicating that there are Stark splits in the emission bands. This phenomenon results from the incorporation of Er^{3+} ions into BaF_2 nanoparticles, which is also found in Er^{3+} -doped NaYF_4 nanocrystals.¹⁹ The full width at half maximum (FWHM) of the spectra is 151 nm, 79 nm, 83 nm, and 81 nm for uncoated nanoparticles, PMMA coated nanoparticles, uncoated nanoparticles/PMMA composites and PMMA coated nanoparticles/PMMA composites, respectively. The difference of spectral width can be attributed to the particle size and surface modification. On one hand, the bigger particle size results in the smaller FWHM, a result observed in our previous work.²⁰ On the other hand, the uneven broadening can also affect the FWHM.²¹ The unsaturated band and imperfection on the

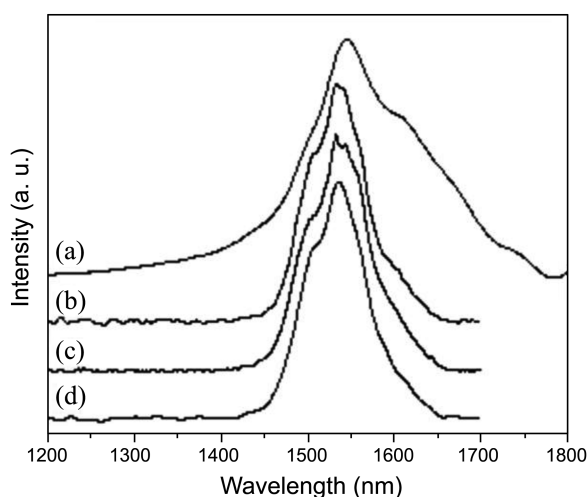


Figure 4. Photoluminescence spectra of uncoated nanoparticles (a), PMMA coated nanoparticles (b), uncoated nanoparticles/PMMA composites (c) and PMMA coated nanoparticles/PMMA composites (d).

particle surface induce dispersed energy levels for Er^{3+} , and these dispersed energy levels leads to unevenly-broadened spectrum. For the surface of modified particles coated with PMMA, some of the dispersed energy levels were “limited”, and consequently, the spectrum narrowed.

Conclusion

In conclusion, a novel route of one-step in situ polymerization to synthesize PMMA coated $\text{BaF}_2:\text{Er}^{3+}$ nanoparticle has been developed. The PMMA coated particle is about 20 nm and can be well dispersed in a polymer matrix compared to uncoated particles. The FWHM of emission spectral of coated particles is about 79 nm, narrower than that of uncoated particles. Although the FWHM of coated particles/PMMA composites is smaller than that of uncoated particles/PMMA, it can reach 81 nm, which meets the demand of wavelength-division multiplexing system (80 nm).

Acknowledgments. This work is financially supported by FCT (PTDC/CTM/108975/2008, SFRH/BPD/44561/2008). National Basic Research Program of China (2007CB935502), and the National Natural Science Foundation of China (NSFC 50702057). And the publication cost of this paper was supported by the Korean Chemical Society.

References

- Hagenmüller, P. *Inorganic Solid Fluorides: Chemistry and Physics*; Academic Press: New York, 1985.
- Barros, J. R.; Bocker, C.; Rüssel, C. *Solid State Sci.* **2010**, *12*, 2086.
- Kumar, K. U.; Babu, P.; Jang, K. H.; Seo, H. J.; Jayasankar, C. K.; Joshi, A. S. *J. Alloys Compds.* **2008**, *458*, 509.
- Wojtowicz, A. *J. Opt. Mater.* **2009**, *31*, 1772.
- Kumar, G. A.; Riman, R.; Chae, S. C.; Jang, Y. N.; Bae, I. K.; Moon, H. S. *J. Appl. Phys.* **2004**, *95*, 3243.
- Beecroft, L. L.; Ober, C. K. *Chem. Mater.* **1997**, *9*, 13027.
- Malitson, I. H. *J. Opt. Soc. Am.* **1964**, *54*, 628.
- Slooff, L. H.; van Blaaderen, A.; Polman, A.; Hebbink, G. A.; Klink, S. I.; Van Veggel, F. C. J. M.; Reinhoudt, D. N.; Hofstraat, J. W. *J. Appl. Phys.* **2002**, *91*, 3955.
- Ruckenstein, E.; Park, J. S. *Polymer* **1992**, *33*, 405.
- Li, R. K. Y.; Lu, S. N.; Choy, C. L. *J. Thermoplast Compos. Mater.* **1995**, *8*, 304.
- Lu, S. N.; Yan, L.; Zhu, X. G.; Qi, Z. N. *J. Mater. Sci.* **1992**, *27*, 4633.
- Lian, H. Z.; Ye, Z. R.; Shi, C. S. *Nanotechnology* **2004**, *15*, 1455.
- Lian, H. Z.; Liu, J.; Ye, Z. R.; Shi, C. S. *Chem. Phys. Lett.* **2004**, *386*, 291.
- Porta, F.; Prati, L.; Rossi, M.; Scari, G. *Colloids and Surfaces A: Physicochem. Eng. Aspects* **2002**, *211*, 43.
- Hou, S. Y.; Xing, Y.; Liu, X. C.; Zou, Y. C.; Liu, B.; Sun, X. J. *CrystEngComm* **2010**, *12*, 1945.
- Bender, C. M.; Burlitch, J. M. *Chem. Mater.* **2000**, *12*, 1969.
- Tikhomirov, V. K.; Furniss, D.; Seddon, A. B.; Reaney, I. M.; Beggiora, M.; Ferrari, M.; Montagna, M.; Rolli, R. *Appl. Phys. Lett.* **2002**, *81*, 1937.
- Chen, D. H.; Wu, S. H. *Chem. Mater.* **2000**, *12*, 1354.
- Liu, F.; Ma, E.; Chen, D. Q.; Wang, Y. S.; Yu, Y. L.; Huang, P. *J. Alloys Compds.* **2009**, *467*, 317.
- Lian, H. Z.; Liu, J.; Ye, Z. R.; Shi, C. S. *J. Nanosci. Nanotechnol.* **2008**, *8*, 1380.
- Macfarlane, R. M.; Shelby, R. M. *Opt. Commun.* **1983**, *45*, 46.